Repeatability of Radiotracer Uptake in Normal Abdominal Organs with ^{111}In-Pentetreotide Quantitative SPECT/CT

Steven P. Rowe*, Esther Vicente*, Nadège Anizan, Hao Wang, Jeffrey P. Leal, Martin A. Lodge, Eric C. Frey, and Richard L. Wahl

The Russell H. Morgan Department of Radiology and Radiological Science, Johns Hopkins University School of Medicine, Baltimore, Maryland

With an increasing emphasis on quantitation of SPECT imaging and its use in dosimetry to guide therapies, it is desirable to understand the repeatability in normal-organ SPECT uptake values (SPECT-UVs). We investigated the variability of normal abdominal organ uptake in repeated ^{111}In-pentetreotide SPECT studies. **Methods:** Nine patients with multiple ^{111}In-pentetreotide SPECT/CT studies for clinical purposes were evaluated. Volumes of interest were drawn for the abdominal organs and applied to SPECT-UVs. The variability of those values was assessed. **Results:** The average SPECT-UV for the liver (1.7 ± 0.6) was much lower than for the kidneys (right, 8.0 ± 2.4; left, 7.5 ± 1.7). Interpatient and intrapatient variability was similar (intraclass correlation coefficients, 0.40–0.59) for all organs. The average coefficients of variation for each organ for each patient were obtained and averaged across all patients (0.26 for liver, 0.22 for right kidney, and 0.20 for left kidney). The coefficients of variation for the organs across all scans were 0.33 (liver), 0.30 (right kidney), and 0.22 (left kidney). **Conclusion:** Variability across all patients and all scans for the liver was higher than reported with ^{18}F-FDG PET, though left kidney variability was similar to PET liver variability and left kidney uptake may be able to serve as an internal metric for determining the quantifiability of an ^{111}In-pentetreotide SPECT study.

Key Words: quantitative SPECT; ^{111}In-pentetreotide SPECT; SPECT-UV; dosimetry

J Nucl Med 2015; 56:985–988
DOI: 10.2967/jnumed.115.155358

SPECT has come to play an important role in the evaluation of numerous medical conditions, oncologic disease states, and normal physiology and can be used in place of or addition to planar imaging as a problem-solving tool. SPECT can better characterize findings and can detect additional lesions not seen on planar imaging by combining the functional information from single-photon imaging with the anatomic information from CT in 3 dimensions (*1*,*2*). The combination of SPECT and CT (SPECT/CT) allows us to further refine the anatomic and diagnostic specificity of SPECT and provide attenuation correction to improve quantitative accuracy.

Received Feb. 3, 2015; revision accepted Apr. 15, 2015.
For correspondence or reprints contact: Richard L. Wahl, Washington University School of Medicine, Department of Radiology, Campus Box 8131, 660 S. Euclid Ave., St. Louis, MO 63110.
E-mail: wahlr@mir.wustl.edu
*Contributed equally to this work.
Published online May 14, 2015.

An important aspect of oncology imaging is assessing tumor response or progression before and while the patient is undergoing therapy. An emerging role of SPECT is quantifying in absolute terms the uptake of radiotracers in normal tissues and tumors to help guide radiopharmaceutical therapies. Although this can be performed qualitatively, it may be desirable to perform these functions in a strictly quantitative sense.

Quantitation has already become widely accepted for both anatomic imaging (Response Criteria in Solid Tumors (*3*)) and PET (PET response criteria in solid tumors [PERCIST] (*4*)). Quantitation of treatment response by SPECT and dosimetry will likely grow in importance as tumor-specific tracers for diagnosis and radiopharmaceutical treatment are increasingly applied in practice.

SPECT remains widely thought of as an intrinsically nonquantitative or semiquantitative modality (*5*). However, in addition to the ability of SPECT/CT systems to perform attenuation compensation, methods that compensate for scatter and the collimator-detector response (i.e., the distance-dependent blurring due to the finite acceptance angle of collimator holes and the detector intrinsic resolution) have been developed (*6*–*12*). On the basis of these developments, several groups have reported quantitative approaches to many commonly imaged SPECT radionuclides relevant to cancer imaging including ^{111}In (*10*) and ^{99m}Tc (*13*).

Measurements of tumor uptake values above diagnostic thresholds from a single image or measurements of changes in tumor uptake in sequential images to assess response are only meaningful to the extent that they are larger than the intrinsic variability of the measurement. Similarly, the reliability of the prediction of the radiation-absorbed dose from a therapeutic administration of a radiopharmaceutical to tumor or normal organs from the SPECT/CT distribution of a diagnostic administration depends on the reliability of the SPECT/CT measurement. An important component of this reliability is the intrinsic variability in the estimate of in vivo activity distributions as measured by SPECT/CT. The goal of this work was to provide an initial characterization of the variability of normal abdominal organ uptake in patients undergoing multiple ^{111}In-pentetreotide (OctreoScan; Mallinckrodt Pharmaceuticals) SPECT/CT examinations.

MATERIALS AND METHODS

This retrospective study was approved by the Institutional Review Board at our hospital. Chart review was used to select 9 patients who had between two and three ^{111}In-pentetreotide SPECT/CT studies. Each patient had a history of neuroendocrine or carcinoid tumor, and the studies had been clinically indicated for monitoring for disease progression or response to therapy. Table 1 presents selected demographic and clinical information for each patient.

TABLE 1
Selected Demographic and Clinical Information for Patients Included in This Study

Patient	Sex	Age range during which scans were acquired (y)	Creatinine levels at time scans were acquired (mg/dL)	No. of scans	Tumor type	Relevant prior surgery	Additional therapies before imaging
1	F	60–65	0.6–0.8	2	Pancreatic neuroendocrine	Distal pancreatectomy, splenectomy, partial hepatectomy	Chemoembolization, ^{90}Y therapy
2	M	63–67	0.8–1.0	2	Pancreatic neuroendocrine	Distal pancreatectomy	NA
3	M	66	0.8	2	Small bowel neuroendocrine	N/A	NA
4	F	71–72	0.6–0.8	2	Pancreatic neuroendocrine	Whipple procedure (pancreatico-duodenectomy)	Radiofrequency ablation of liver metastasis
5	F	58	0.6	2	Pancreatic neuroendocrine	Distal pancreatectomy, splenectomy, liver wedge resection	Chemoembolization
6	M	61–65	Not available	3	Small bowel carcinoid	Small bowel resection	NA
7	F	36–37	0.6–0.9	2	Mediastinal neuroendocrine	Mediastinal, pleural, and diaphragmatic resections	NA
8	F	61–63	0.8–0.9	2	Pancreatic neuroendocrine	Distal pancreatectomy, splenectomy	NA
9	F	46–51	0.8	3	Small bowel carcinoid	Liver wedge resections	Radiofrequency ablation of liver metastases

N/A = not applicable.

Images were acquired on a Precedence 16-slice SPECT/CT scanner (Philips) nominally 24 h after intravenous injection of 229 ± 19 MBq (6.2 ± 0.5 mCi) of ^{111}In-pentetreotide. The acquisitions were performed with two 20%-wide energy windows centered at 171 and 245 keV. The duration of SPECT acquisitions was 48 min, and projections were acquired into 128 × 128 matrices with a pixel size of 0.466 cm at 128 projections over 360°. The images were reconstructed using 3 iterations of 16 subsets of an ordered-subset expectation maximization algorithm. The reconstructions included Philips' clinical attenuation correction and model-based scatter compensations. After reconstruction, the images were filtered with a fifth order 3-dimensional Butterworth filter with a cutoff frequency of 0.65 cycles per pixel. CT images were obtained using standard clinical parameters for noncontrast CT scans, typically 120 kVp, 80–160 mA (weight-dependent), gantry rotation speed of 0.5 s, and pitch of 0.9.

Volumes of interest (VOIs) were drawn on a commercial workstation (Mirada Medical) encompassing the liver and kidneys in each patient on the basis of visual estimates of the organ edges in the SPECT images. The CT images were available for localization and determination of any relevant postoperative changes, but the CT images were not otherwise used in determining the VOIs. Because multiple patients were postsplenectomy (Table 1), an analysis of the spleen was not performed.

The SPECT-UVs were calculated using:

$$\text{SPECT-UV} = \frac{\text{Counts}_{\text{organ}}/\text{F}_{\text{calib}} \times \text{time}_{\text{acquisition}}}{\text{Activity}_{\text{dc}}/\text{Weight}_{\text{patient}}}, \qquad \text{Eq. 1}$$

where $\text{Counts}_{\text{organ}}$ (c/cc) are the measured average counts per cc inside the organ VOI; F_{calib} (cps/Bq) is the calibration factor to convert the counts in the VOI to activity; $\text{time}_{\text{acquisition}}$ (s) is the duration of the acquisition; $\text{Activity}_{\text{dc}}$ (Bq) is the total radiotracer activity injected into the patient (dc: decay corrected to the time of acquisition); and $\text{Weight}_{\text{patient}}$ (g) is the weight of the patient in grams, used here to estimate the volume, assuming the average density of the patient as 1 g/cc.

F_{calib} was calculated using SPECT data from a cylinder (diameter, 23 cm; height, 27.4 cm) filled with a solution containing 365.2 MBq (9.89 mCi) of ^{111}In. Image acquisition and reconstruction parameters were the same as those used for the patients. The total of the counts in the reconstructed image of the phantom was determined inside a VOI defined manually to include all counts in the phantom. This larger VOI was used to reduce the impact of partial-volume effects. The value of F_{calib} was calculated as the total measured counts in the image of the cylinder divided by the product of the known activity

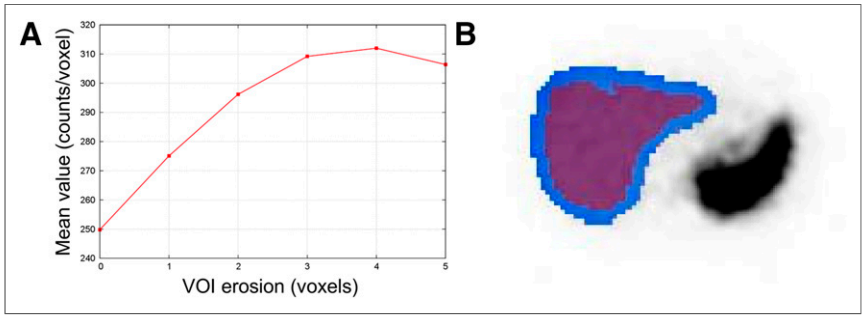

FIGURE 1. Average counts per voxel as function of number of voxels peripherally eroded from representative liver VOI (A), with uneroded VOI (blue) and 3-voxel eroded VOI (purple) shown overlying axial SPECT image (B).

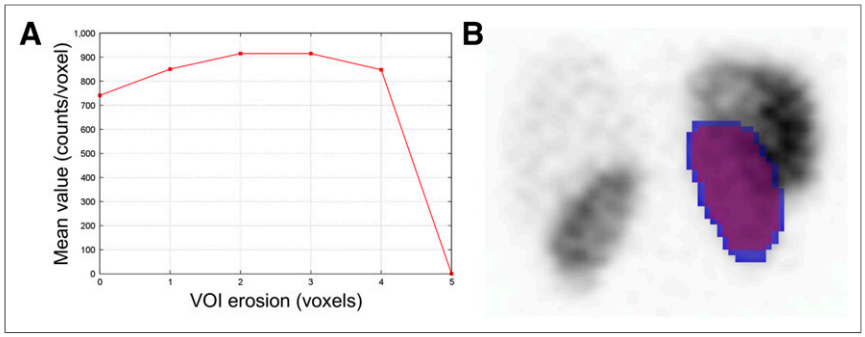

FIGURE 2. Average counts per voxel as function of number of voxels peripherally eroded from example left kidney VOI (A), with uneroded VOI (blue) and 1-voxel eroded VOI (purple) shown overlying coronal SPECT image (B).

and the total acquisition duration. We compared the calibration factor determined this way to one measured using a sphere in a cylinder and a syringe in air and found the difference to be less than 1%.

From the multiple measures of SPECT-UV over time within a subject, intraclass correlation coefficients (ICCs (*14*)) and coefficients of variation (COVs) across scans for the same patient and across all scans from all patients were calculated.

RESULTS

The VOIs were noted to have gradually decreasing uptake along the organ peripheries, likely due to edge partial-volume effects. Thus, the organ VOIs were peripherally eroded by increments of 1 voxel until a peak in the average organ uptake was reached. The uptake at the peak was used as it was less influenced by edge partial-volume effects. For the liver, a peripheral erosion of 3 voxels was used. Figure 1 shows a representative example of the original and eroded whole-organ liver VOIs. In the case of the kidneys, the used erosion was 1 voxel (Fig. 2).

In 3 of the patients in this study with pancreatic neuroendocrine tumors, metastatic disease to the liver developed. In 1 of these patients, uptake to the liver was diffusely increased (MR imaging demonstrated diffuse metastatic disease to the liver parenchyma). The liver from that scan was excluded from analysis. For the other 2 patients, discrete lesions with increased radiotracer uptake were visually apparent, and the VOIs were defined to exclude the tumors.

The average SPECT-UVs for the liver, left kidney, and right kidney from each scan are displayed in Figure 3. The average SPECT-UVs and their 95% confidence intervals were calculated for the eroded VOIs for the liver, left kidney, and right kidney and were compiled across all studies (Table 2). As expected from visual assessments, there was high renal parenchymal uptake of ^{111}In-pentetreotide. The mean ± SD SPECT-UVs were 7.5 ± 1.7 (range, 4.8–9.4) for the left kidney and 8.0 ± 2.4 (range, 3.8–10.2) for the right kidney. These values were much higher than the corresponding SPECT-UVs for the liver (1.7 ± 0.6 [range, 0.8–2.6]). The average SPECT-UVs for the left and right kidneys were similar, implying a high degree of spatial reliability within the reconstructed images.

The ICCs and COVs of the eroded whole-organ volumes are also included in Table 2. Of note, the ICCs were all in a relatively narrow range around 0.5, indicating nearly equal intrapatient and interpatient variability. The COVs for the organ VOIs on an intrapatient basis—that is, the COV for each patient averaged across all patients—revealed a trend toward higher variability in the liver than the kidneys (0.26 ± 0.14 [range, 0.11, 0.55] for the liver, 0.20 ± 0.07 [range, 0.07–0.31] for the left kidney, and 0.22 ± 0.09 [range, 0.03–0.33] for the right kidney). When the COVs were calculated on an interpatient basis across all patients, variability in the liver (0.33) and right kidney (0.30) was higher than in the left kidney (0.22).

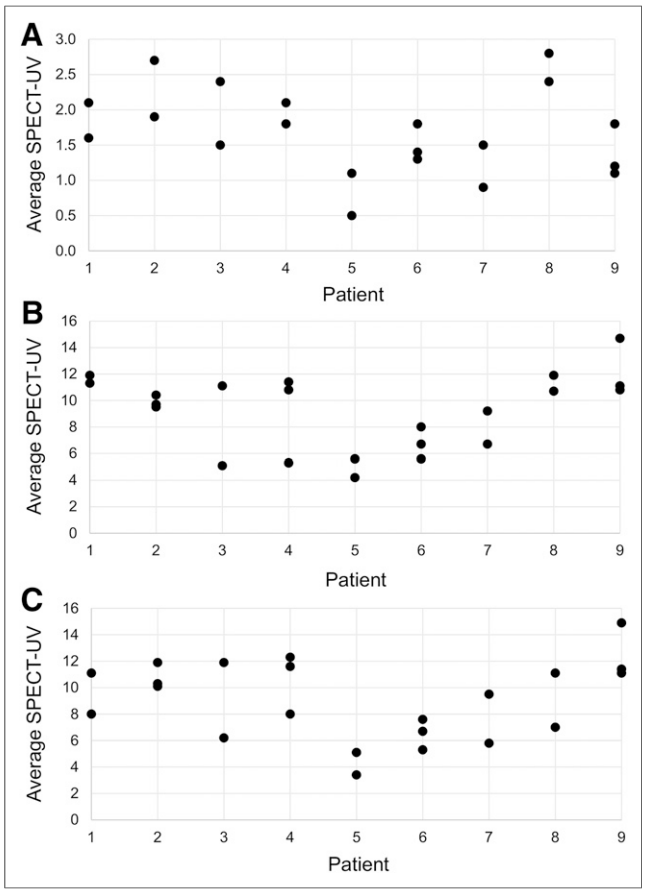

FIGURE 3. Distribution of average SPECT-UVs for liver (A), left kidney (B), and right kidney (C) in each patient.

DISCUSSION

It is important to define the ability of SPECT to function as a quantitative modality to most effectively monitor the disease status and response to therapy of oncology patients. Predicting the radiation-absorbed dose of a therapeutic radiopharmaceutical from diagnostic and posttreatment SPECT images is of growing importance. Many tumors remain uniquely evaluable by SPECT radiotracers, and SPECT agents are often used in organ dosimetry.

An in-depth understanding of the uptake parameters of the radiotracers used in SPECT, such as intrinsic organ uptake variability, is needed to fully implement quantitative SPECT evaluation of tumors and their response to therapy. Normal-organ radiotracer accumulation as a tool to calculate the radiation-absorbed dose is also important. In this work, we have demonstrated that the

TABLE 2
Average SPECT-UV, ICCs, and COVs for Each Patient Averaged Over All Patients, and COVs Across All Scans for Liver, Left Kidney, and Right Kidney

Organ	Average SPECT-UV ± SD	ICC	COV
Liver	1.7 ± 0.6 (0.8–2.6)	0.59	0.33
Left kidney	7.5 ± 1.7 (4.8–9.4)	0.50	0.22
Right kidney	8.0 ± 2.4 (3.8–10.2)	0.40	0.30

Data in parentheses are ranges.

variability in normal-organ uptake across all scans from all patients appears greater than the comparable variability in PET (COV of 0.33 for the liver SPECT-UV vs. 0.21 for ^{18}F-FDG PET (*15*)). However, the overall variability of uptake in the left kidney in this study (COV, 0.22) was actually quite similar to the reported ^{18}F-FDG PET liver variability.

Uptake in the liver was chosen as the basis of whether a PET study could be reliably quantified given its moderate parenchymal ^{18}F-FDG uptake and the low variability of that uptake across sequential scans. In the context of ^{111}In-pentetreotide, the left kidney may provide a measure of the suitability for quantitation (quantifiability) of a study in a manner similar to the liver in sequential ^{18}F-FDG PET studies as assessed by PERCIST 1.0. The seemingly lower variability of the left kidney in comparison to the right (COV, 0.30) may be caused by crosstalk between activity estimates in the liver and left kidney due to partial-volume effects.

Patient-specific and scan-specific sources of variability were nearly equal (ICCs, 0.40–0.59). These findings suggest that scan-specific normal-organ uptake parameters may be desirable for assessing the quantifiability of normal tissue and tumor uptake values.

We encountered 2 technical limitations in the process of calculating the SPECT-UVs: patient weights were not consistently recorded at the time of imaging, and exact injection times were not available in the medical record for some scans. We thus estimated some patient weights from chart review and some acquisition start times based on the scheduled study start time. In the case of ^{111}In (half-life, 2.80 d), errors due to start time discrepancies would be small. As quantitative SPECT becomes clinically more accepted, stricter imaging protocols and data recording standards will be necessary.

One source of variability in the measurements is camera variations in camera sensitivity over time. However, recent data indicate that camera variability over time is less than 1% (*16,17*).

CONCLUSION

In patients with repeated ^{111}In-pentetreotide SPECT studies, left kidney SPECT-UV variability was similar to liver SUV variability previously described with ^{18}F-FDG PET. This similarity suggests that left kidney uptake measurements may serve as an internal metric for determining the quantifiability of an ^{111}In-pentetreotide SPECT scan.

DISCLOSURE

The costs of publication of this article were defrayed in part by the payment of page charges. Therefore, and solely to indicate this fact, this article is hereby marked "advertisement" in accordance with 18 USC section 1734. Funding for this study was provided by National Institutes of Health grants U01 CA140204, T32-EB010021-05, T32 EB006351, and R01 CA109234. No other potential conflict of interest relevant to this article was reported.

ACKNOWLEDGMENT

We thank Judy Buchanan for editorial assistance.

REFERENCES

1. Sedonja I, Budihna NV. The benefit of SPECT when added to planar scintigraphy in patients with bone metastasis in spine. *Clin Nucl Med.* 1999;24:407–413.
2. Jacene HA, Goetze S, Patel H, Wahl RL, Ziessman HA. Advantages of hybrid SPECT/CT vs SPECT alone. *Open Med Imag J.* 2008;2:67–79.
3. Eisenhauer EA, Therasse P, Bogaerts J, et al. New response evaluation criteria in solid tumours: revised RECIST guideline (version 1.1). *Eur J Cancer.* 2009;45:228–247.
4. Wahl RL, Jacene H, Kasamon Y, Lodge MA. From RECIST to PERCIST: evolving considerations for PET response criteria in solid tumors. *J Nucl Med.* 2009;50(suppl 1):122S–150S.
5. Bailey DL, Willowson KP. An evidence-based review of quantitative SPECT imaging and potential clinical applications. *J Nucl Med.* 2013;54:83–89.
6. Chang LT. A method for attenuation correction in radionuclide computed tomography. *IEEE Trans Nucl Sci.* 1978;NS-25:638–643.
7. Frey EC, Tsui BMW. A new method for modeling the spatially-variant, object-dependent scatter response function in SPECT. *IEEE.* 1996;2:1082–1086.
8. Beekman FJ, Kamphuis C, Frey EC. Scatter compensation methods in 3D iterative SPECT reconstruction: a simulation study. *Phys Med Biol.* 1997;42:1619–1632.
9. El Fakhri G, Buvat I, Benali H, Todd-Pokropek A, Di Paola R. Relative impact of scatter, collimator response, attenuation and finite spatial resolution corrections in cardiac SPECT. *J Nucl Med.* 2000;41:1400–1408.
10. He B, Du Y, Song X, Segars WP, Frey EC. A Monte Carlo and physical phantom evaluation of quantitative In-111 SPECT. *Phys Med Biol.* 2005;50:4169–4185.
11. Cheng L, Hobbs RF, Segars PW, Sgouros G, Frey EC. Improved dose-volume histogram estimates for radiopharmaceutical therapy by optimizing quantitative SPECT reconstruction parameters. *Phys Med Biol.* 2013;58:3631–3647.
12. Rong X, Frey EC. A collimator optimization method for quantitative imaging: application to Y-90 bremsstrahlung SPECT. *Med Phys.* 2013;40:082504.
13. Willowson K, Bailey DL, Baldock C. Quantitative SPECT using CT-derived corrections. *Phys Med Biol.* 2008;53:3099–3112.
14. Shrout PE, Fleiss JL. Intraclass correlations: uses in assessing rater reliability. *Psychol Bull.* 1979;86:420–428.
15. Perry K, Tann M, Miller M. Which reference tissue is best for semiquantitative determination of FDG activity [abstract]? *J Nucl Med.* 2008;49(suppl 1):425P.
16. Anizan N, Wang H, Zhou XC, Hobbs RF, Wahl RL, Frey EC. Factors affecting the stability and repeatability of gamma camera calibration for quantitative imaging applications based on a retrospective review of clinical data. *EJNMMI Res.* 2014;4:67–77.
17. Anizan N, Wang H, Zhou XC, Wahl RL, Frey EC. Factors affecting the repeatability of gamma camera calibration for quantitative imaging applications using a sealed source. *Phys Med Biol.* 2015;60:1325–1337.